Density fluctuations and field mixing in the critical fluid

1992 J. Phys.: Condens. Matter 4 3087

(http://iopscience.iop.org/0953-8984/4/12/008)

J. Phys.: Condens. Matter 4 (1992) 3087–3108. Printed in the UK

Density fluctuations and field mixing in the critical fluid

N B Wilding and A D Bruce
Department of Physics, The University of Edinburgh, Edinburgh EH9 3JZ, UK

Received 20 November 1991

Abstract. We develop a finite-size-scaling theory describing the joint density and energy fluctuations in a near-critical fluid. As a result of the mixing of the temperature and chemical potential in the two relevant scaling fields, the energy operator features in the critical density distribution as an antisymmetric correction to the limiting scale-invariant form. Both the limiting form and the correction are predicted to be functions that are characteristic of the Ising universality class, and are independently known. The theory is tested with extensive Monte Carlo studies of the two-dimensional Lennard-Jones fluid, within the grand canonical ensemble. The simulations and scaling framework together are shown to provide a powerful way of identifying the location of the liquid-gas critical point, while confirming and clarifying its essentially Ising character. The simulations also show a clearly identifiable signature of the field-mixing responsible for the failure of the law of rectilinear diameter.

1. Introduction

Within the contemporary framework, the theoretical problems posed by a given continuous phase transition fall naturally into two categories. First one may wish to establish the universality class [1] to which the phase transition belongs, thereby identifying the values of the universal quantities characterizing the critical behaviour. Second one may wish to determine the set of non-universal quantities (notably those that locate the critical point, and the associated relevant scaling fields) in terms of the parameters describing the microscopic interactions. Notwithstanding its familiarity, the continuous phase transition associated with the liquid-gas critical point of the simple fluid continues to pose problems in both categories: we consider them in turn.

It has been both long and widely believed [2] that the liquid-gas critical point falls into the universality class of the simple Ising model, the default for systems with short-range interactions and a scalar order parameter. There is substantial circumstantial evidence supporting this view [3]: the measured values of the liquid-gas critical indices are, it now seems generally agreed, quite consistent with the values emerging from both series expansion studies of the three-dimensional lattice Ising model, and renormalization group studies of its continuum counterpart. The direct evidence is less satisfying. Analytic studies have focused on a partially phenomenological Landau–Ginsburg–Wilson Hamiltonian incorporating 'odd' terms to reflect the absence of particle–hole symmetry characteristic of real fluids: expansions in $4 - d$ show [4, 5] that such terms constitute perturbations that are irrelevant with respect to the conventional Ising fixed point of the renormalization group, suggesting that the Ising behaviour does indeed survive the lowered symmetry, at least 'near' dimension $d = 4$. However the 'path' (renormalization group flow process) that connects

0953-8984/92/123087+22$04.50

a realistic microscopic fluid model Hamiltonian to the Ising fixed point form (in physical dimensions!) remains largely unexplored, and its very existence open to question [6]†. As regards computer-simulation determination of the universal critical behaviour, there is, to our knowledge, no work remotely comparable with the work on lattice models.

The extent of the current knowledge of *non*-universal features of the critical behaviour in even the simplest model fluids is also severely limited by the dearth of large-scale simulations conducted with an understanding of the problems posed by the critical region. Thus, for example, studies of the prototype model fluid (the two-dimensional Lennard-Jones model, also the subject of the present work), have yielded [7–10] wildly varying assignments of the critical temperature, largely (we believe) because of a failure to appreciate the scale and character of finite-size effects. Moreover, none of these studies has attempted to explore the physical character of the relevant scaling fields, which (it has long been appreciated [11]) should comprise *mixtures* of the chemical potential and the temperature. This 'mixing', a manifestation of particle–hole asymmetry, is a fundamental issue in the theory of critical fluids. Its most widely celebrated signature—the failure of the 'law of rectilinear diameter' [11]—has elicited considerable experimental activity [12–16]. While there is some understanding of the microscopic factors controlling the size of the effect [17–19], little attention seems to have been given to whether it might have some other signature, more accessible to simulation experiments.

Two recent papers have made some inroads into at least some of these problems.

First, Reatto *et al* [20] have developed a computational formalism, originally set out some time ago [21], having a renormalization-group flavour, and with the potential to predict both universal and non-universal critical-point parameters. The results are numerically impressive. However the approach seems to rely implicitly on a small '$4 - d$' approximation, and, because of the originality of its formulation, does less than one might wish to illuminate the respects in which the fluid 'belongs' to the Ising universality class.

By contrast, the work of Rovere *et al* [22, 23] is a natural extension to the fluid problem of techniques developed by Binder and others [24, 25] to handle lattice-based problems. The approach involves the Monte Carlo study of the distribution of fluctuations in the *density* of the fluid contained within some *sub-volume* of linear dimension l of a system of linear dimension L, the system itself containing a *fixed* number of particles. Although having the advantages associated with a well established formalism (including the potential to expose the connection with Ising magnets) the results emerging from this study are largely qualitative, in part (we believe) because of the difficulties of handling the *two* length-scales l and L. Moreover, the whole issue of the nature of the scaling fields was not addressed.

The strategy of the present work is close in spirit to that of Rovere *et al* [22, 23] but with significant differences and extensions. Its essential features are as follows‡. We have performed an extensive Monte Carlo study of a two-dimensional fluid of particles interacting through a (truncated) Lennard-Jones potential. The principal motivation for the model is its simplicity: it represents the most computationally tractable system with the credentials (notably the symmetry) of a real fluid. However, notwithstanding

† Note, however, that Zhang and Badiali (1991) have recently provided a field-theoretic renormalization group analysis of the fluid problem, avoiding the Landau–Ginsburg phenomenology, and confirming the stability of the Ising fixed point within a $4 - d$ expansion.

‡ A brief preliminary report of this work has been given elsewhere [26].

its simplicity, the model does have direct experimental relevance for submonolayer systems [27]. We have chosen to work within the *grand canonical* ensemble so that the density of the system *as a whole* is itself a statistical variable, whose distribution we analyse within a finite-size-scaling framework. This approach frees us of the extra length-scale that complicates the ('sub-volume') method of Rovere *et al*, while allowing us to make explicit quantitative contact with studies of the fluctuations of the magnetization in the canonical ensemble of the lattice-based members of the two-dimensional Ising universality class. In the process, we have developed the more general *finite-size-scaling theory* needed to address the interplay of density and *energy* fluctuations, which is an essential corollary of the mixed character of the relevant scaling fields (specifically, the fact that the chemical potential features in the thermal field). We show, in particular, that this mixing manifests itself in a *correction* to the limiting large L behaviour of the critical density distribution. This correction has a *different symmetry* from the asymptotically dominant form (it is an odd function); moreover its form is shown to be prescribed by *independently determined* functions characteristic of the Ising universality class. Accordingly it represents a potentially distinctive signature of the field-mixing.

We summarize the main features of our results. First, we provide good evidence that the critical-point distribution of the fluid *density* matches quantitatively the critical distribution of the *magnetization* of the Ising magnet, thereby confirming the status of the fluid as a member of the Ising universality class, and exposing more fully its meaning. Second, we find that the mapping onto universal Ising-like behaviour sets in at remarkably short length-scales, being evident already in systems containing only (a mean of) the order of 10^2 particles. Third, our results suggest that most previous analyses of this system have significantly *overestimated* the critical temperature as a result of a failure to handle finite-size effects, whose character is graphically exposed by the present analysis. Finally, our results provide substantial corroboration of our extended scaling theory, and show a clear signature of the mixing responsible for the failure of the law of rectilinear diameter.

2. Background

We consider a classical single-component fluid whose configurational energy Φ (which we write in units of $k_B T$) resides in a sum of pairwise interactions amongst the N particles it contains:

$$\Phi(\{r\}) = \sum_{i<j=1}^{N} \phi(|r_i - r_j|). \tag{2.1}$$

The interaction potential ϕ is assigned the Lennard-Jones form

$$\phi(r) = 4w[(\sigma/r)^{12} - (\sigma/r)^6] \tag{2.2}$$

where σ is a parameter which serves to set the interaction range while w measures the well depth (in units of $k_B T$). The fluid is confined to a volume $V = L^d$ (with $d = 2$ in the simulations described later) and is thermodynamically open, so that

both the total energy and the particle number are statistical variables. The associated (grand canonical) partition function takes the form:

$$\mathcal{Z}_L = \sum_{N=0}^{\infty} \prod_{i=1}^{N} \left\{ \int \mathrm{d}\boldsymbol{r}_i \right\} \mathrm{e}^{[\mu N - \Phi(\{\boldsymbol{r}\})]} \tag{2.3}$$

where μ is the chemical potential (in units of $k_B T$).

We shall be concerned with the behaviour of the *number density*

$$\rho = L^{-d} N \tag{2.4a}$$

and the configurational *energy density*

$$u = L^{-d} w^{-1} \Phi(\{\boldsymbol{r}\}) \tag{2.4b}$$

which we write in units of the dimensionless well depth, w. The statistical behaviour of these variables is fully described by their joint probability distribution, defined formally by

$$p_L(\rho, u) = \left\langle \delta \left[\rho - L^{-d} N\right] \delta \left[u - L^{-d} w^{-1} \Phi(\{\boldsymbol{r}\})\right] \right\rangle \tag{2.5a}$$

or, more explicitly,

$$p_L(\rho, u) = L^d \mathcal{Z}_L^{-1} \prod_{i=1}^{N=L^d\rho} \left\{ \int \mathrm{d}\boldsymbol{r}_i \right\} \mathrm{e}^{L^d[\mu\rho - wu]} \delta \left[u - L^{-d} w^{-1} \Phi(\{\boldsymbol{r}\})\right]. \tag{2.5b}$$

We shall focus specifically on the region close to the critical point, which is located (within the grand canonical framework) by critical values μ_c and w_c of the (reduced) chemical potential and well depth. The deviations of these two control parameters from their critical values will control the sizes of the two relevant scaling fields, τ and h, of the fixed point characterizing the critical behaviour [28]. In general (in the absence of the special symmetry prevailing in the Ising ferromagnet) we expect [11] that these scaling fields will comprise *linear combinations* of these deviations:

$$\tau = w_c - w + s(\mu - \mu_c) \qquad h = \mu - \mu_c + r(w_c - w) \tag{2.6}$$

where s and r are system-specific parameters controlling the extent of the mixing, and vanishing identically for systems with the Ising symmetry. Associated with these two scaling fields are the two relevant conjugate operators, $\mathcal{E}$ and $\mathcal{M}$, defined by the requirements that

$$\langle \mathcal{E} \rangle = L^{-d} \partial \ln \mathcal{Z}_L / \partial \tau \qquad \langle \mathcal{M} \rangle = L^{-d} \partial \ln \mathcal{Z}_L / \partial h \tag{2.7}$$

and identifiable in the Ising context as the energy density and magnetization respectively. As a result of the mixed character of the scaling fields, one finds that, in the present context, these operators are *linear combinations* of the energy and number densities:

$$\mathcal{E} = \frac{1}{1 - sr} [u - r\rho] \qquad \mathcal{M} = \frac{1}{1 - sr} [\rho - su]. \tag{2.8}$$

The joint distribution of energy and density is simply related to the joint distribution of the mixed operators:

$$p_L(\rho,u)=\frac{1}{1-s\tau}p_L(\mathcal{M},\mathcal{E}). \tag{2.9}$$

For the limiting near-critical behaviour of this joint distribution we make the following finite-size-scaling *ansatz*:

$$p_L(\mathcal{M},\mathcal{E})\simeq\Lambda_{\mathcal{M}}^{+}\Lambda_{\mathcal{E}}^{+}\tilde{p}_{\mathcal{M},\mathcal{E}}(\Lambda_{\mathcal{M}}^{+}\delta\mathcal{M},\Lambda_{\mathcal{E}}^{+}\delta\mathcal{E},\Lambda_{\mathcal{M}}h,\Lambda_{\mathcal{E}}\tau) \tag{2.10a}$$

where

$$\Lambda_{\mathcal{E}}=a_{\mathcal{E}}L^{\lambda_{\mathcal{E}}}\qquad\Lambda_{\mathcal{M}}=a_{\mathcal{M}}L^{\lambda_{\mathcal{M}}}\qquad\Lambda_{\mathcal{M}}\Lambda_{\mathcal{M}}^{+}=\Lambda_{\mathcal{E}}\Lambda_{\mathcal{E}}^{+}=L^{d} \tag{2.10b}$$

and

$$\delta\mathcal{M}\equiv\mathcal{M}-\langle\mathcal{M}\rangle_c\qquad\delta\mathcal{E}\equiv\mathcal{E}-\langle\mathcal{E}\rangle_c \tag{2.10c}$$

with

$$\lambda_{\mathcal{E}}=1/\nu\qquad\lambda_{\mathcal{M}}=d-\beta/\nu \tag{2.10d}$$

the exponents associated with the two relevant scaling fields. The subscripts c in equations (2.10c) signify that the averages are to be taken at criticality. Given appropriate choices for the non-universal scale factors $a_{\mathcal{M}}$ and $a_{\mathcal{E}}$ (equation (2.10*b*)), we anticipate that the function $\tilde{p}_{\mathcal{M},\mathcal{E}}$ will be universal.

We motivate and qualify these proposals with the following remarks.

First, we note that they constitute a generalization of the finite-size-scaling *ansatz* for the order-parameter (magnetization) distribution in systems with the Ising symmetry [24] which is recovered, in the present framework, with the identifications $\mathcal{M}\to M$ (the magnetization), $\mathcal{E}\to E$ (the energy density), $\tau\to t$ (the reduced temperature), with h the magnetic field, and formal integration over the energy fluctuations to yield:

$$p_L(M)\simeq\Lambda_{\mathcal{M}}^{+}\tilde{p}_{\mathcal{M}}(\Lambda_{\mathcal{M}}^{+}M,\Lambda_{\mathcal{M}}h,\Lambda_{\mathcal{E}}t) \tag{2.11a}$$

where

$$\tilde{p}_{\mathcal{M}}(x,y,z)\equiv\Lambda_{\mathcal{E}}^{+}\int\mathrm{d}\mathcal{E}\,\tilde{p}_{\mathcal{M},\mathcal{E}}(x,\Lambda_{\mathcal{E}}^{+}\delta\mathcal{E},y,z). \tag{2.11b}$$

Equation (2.11*a*) has been well explored. It has a solid renormalization group basis [29], and substantial support from both Monte Carlo studies [30] and explicit renormalization group calculations [31].

Second, it is easily checked that equation (2.10*a*) is consistent with the standard theory of fluctuations in macroscopic systems [32] according to which (in the regime in which the system size L is large compared with the correlation length ξ, realized here when $\Lambda_{\mathcal{E}}\tau\gg 1$) the operators $\mathcal{M}$ and $\mathcal{E}$ will be Gaussian-distributed about their mean values, with variance controlled by an appropriate response function (order-parameter susceptibility, or specific heat).

Third, and more specifically, it is readily shown that equation (2.10*a*) leads to a coexistence curve diameter ρ_d (the mean of the densities of the two phases which coexist on the $h = 0$ line, for $\tau < 0$) displaying an energy-like singularity, and with an amplitude proportional to the parameter s controlling the extent to which the chemical potential μ contributes to the scaling field τ:

$$\rho_d - \rho_c \sim s|t|^{1-\alpha} \tag{2.12}$$

where $\rho_c \equiv \langle\rho\rangle_c$, and we have made use of standard scaling relations. This is the behaviour anticipated in scaling theories of the fluid free-energy or equation of state [11, 19] which are implicit in equation (2.10*a*).

Finally we must express some caution about the claims which equation (2.10*a*) makes in regard to the spectrum of fluctuations of the 'energy' operator. These claims are substantially less well founded than are those that pertain to the fluctuation spectrum of the 'order parameter'. In the tradition of scaling theories, and, indeed, in keeping with the manner in which equation (2.11*a*) was originally suggested [24], this extended scaling proposal is made on phenomenological grounds, some of which feature in a discussion of the energy spectrum at first-order transitions to be found in [33]. We remark that we would *not* expect the extended theory to hold unless the 'energy' operator is, like the 'order parameter', a strongly fluctuating quantity, whose signature is a divergent specific heat: it is only in these circumstances that it can be consistent to write a scaling form that captures the 'singular' behaviour of the coexistence curve diameter identified in equation (2.12), but not the 'analytic' term that is actually widely observed, often to the exclusion of the non-analytic contribution. The situation we consider explicitly in the course of the simulations only barely satisfies this criterion: the specific heat is only *logarithmically* divergent in the $d = 2$ Ising universality class [34]; even this situation almost certainly calls for an elaboration of equation (2.10*a*), since such logarithmic behaviour is known to involve contributions which, in other circumstances would be dismissed as analytic background (see, e.g., [35]). We have not attempted to construct that more elaborate form—in part, at least because the extended scaling *ansatz* (2.10*a*) turns out to offer a remarkably successful account of our simulations, which involve the energy spectrum only in the limited way we proceed to describe.

Our specific concern is with the distribution of the fluid number density, which follows from equations (2.5*a*), (2.8), (2.9) and (2.10*a*)

$$p_L(\rho) = \int \mathrm{d}u\, p_L(\rho, u)$$

$$\simeq \Lambda_{\mathcal{M}}^{+}\Lambda_{\mathcal{E}}^{+} \int \mathrm{d}\mathcal{E}\, \tilde{p}_{\mathcal{M},\mathcal{E}}(\Lambda_{\mathcal{M}}^{+}[\rho - \rho_c - s\delta\mathcal{E}], \Lambda_{\mathcal{E}}^{+}\delta\mathcal{E}, \Lambda_{\mathcal{M}}h, \Lambda_{\mathcal{E}}\tau). \tag{2.13}$$

Now the structure of our proposed scaling form (2.10*a*) shows that at (or close to) criticality the typical size of fluctuations in the energy-like operator, $\delta\mathcal{E}$, will vary with system size L as $[\Lambda_{\mathcal{E}}^{+}]^{-1} = L^{-(1-\alpha)/\nu}$, while the typical scale of the ordering operator fluctuation, $\delta\mathcal{M}$ will vary as $[\Lambda_{\mathcal{M}}^{+}]^{-1} = L^{-\beta/\nu}$. It follows that, to within corrections that are down on the leading term we retain by of order $L^{-(1-\alpha-\beta)/\nu}$, we may *neglect* the contribution of the energy fluctuations to the first argument of the function $\tilde{p}_{\mathcal{M},\mathcal{E}}$ in equation (2.13). One may *then* proceed to perform the integration on $\mathcal{E}$ to yield a result of the form

$$p_L(\rho) \simeq \Lambda_{\mathcal{M}}^{+}\tilde{p}_{\mathcal{M}}(\Lambda_{\mathcal{M}}^{+}[\rho - \rho_c], \Lambda_{\mathcal{M}}h, \Lambda_{\mathcal{E}}\tau) \tag{2.14}$$

where $\tilde{p}_{\mathcal{M}}(x, y, z)$ is the function identified in equation (2.11*a*) prescribing the Ising magnetization distribution. We conclude then that, to within terms representing corrections to the leading finite-size-scaling behaviour, the reduced symmetry of the fluid manifests itself in the number-density distribution only through the mixed character of the scaling fields (2.6)

Equation (2.14) is the key result for what follows. We will check and exploit its consequences *at* and, to a more limited degree, *close to* the fluid critical point.

Precisely at criticality equation (2.14) implies simply (appealing to (2.10*b*)):

$$p_L(\rho) \simeq a_{\mathcal{M}}{}^{-1} L^{\beta/\nu} \tilde{p}^{\star}_{\mathcal{M}} \left(L^{\beta/\nu} a_{\mathcal{M}}{}^{-1} [\rho - \rho_c] \right) \tag{2.15}$$

where

$$\tilde{p}^{\star}_{\mathcal{M}}(x) = \tilde{p}_{\mathcal{M}}(x, y = 0, z = 0) \tag{2.16}$$

is a function describing the universal and statistically scale-invariant configurations characteristic of the critical point. The form of this function has been well established in studies of the two-dimensional spin-$\frac{1}{2}$ Ising model and its claim to describe other members of this universality class vindicated by studies of the spin-1 Ising model and the ϕ^4 model [30]. We note that this function is *even* (describing, in the magnetic context, the critical fluctuations of the magnetization). The fluid density distribution clearly does not in general have a corresponding symmetry. Accordingly the claim that the critical density fluctuations can be described by (2.15) is remarkable, even by the norms of universal phenomena.

The consequences of equation (2.14) for the behaviour *near* criticality are most readily explored through the implied forms of the *derivatives* of $p_L(\rho)$ with respect to the well-depth parameter w (controlling the effective temperature), and the chemical potential. Appealing to the formal representation provided by equation (2.5*a*) we find

$$\frac{\partial p_L(\rho)}{\partial \mu} = L^d \left[\rho - \langle \rho \rangle \right] p_L(\rho) \tag{2.17a}$$

and

$$\frac{\partial p_L(\rho)}{\partial w} = -L^d \left[\langle u(\rho) \rangle - \langle u \rangle \right] p_L(\rho) \tag{2.17b}$$

where $\langle u(\rho) \rangle$ is the mean energy density for a given ρ. The first of these results provides assistance in refining assigned locations of coexistence and criticality (as described in the discussion of the simulations later). The second result fulfils a similar function, but in addition furnishes a further testable relation. Specifically, appealing to our proposed scaling form (2.14), together with the w-dependence of the scaling fields recorded in (2.6) (and (2.8)) and feeding the consequences into (2.17*b*), we obtain at criticality (where $\langle u \rangle \equiv u_c$)

$$\langle u(\rho) \rangle - u_c \simeq L^{-d} \left\{ r \Lambda_{\mathcal{M}} \tilde{p}^{(1,0)}_{\mathcal{M}} (\Lambda^{+}_{\mathcal{M}} [\rho - \rho_c]) + \Lambda_{\mathcal{E}} \tilde{p}^{(0,1)}_{\mathcal{M}} (\Lambda^{+}_{\mathcal{M}} [\rho - \rho_c]) \right\} \tag{2.18}$$

where

$$\tilde{p}^{(1,0)}_{\mathcal{M}}(x) = \left. \frac{\partial \ln \tilde{p}_{\mathcal{M}}(x, y, 0)}{\partial y} \right|_{y=0} \tag{2.19a}$$

$$\tilde{p}^{(0,1)}_{\mathcal{M}}(x) = \left. \frac{\partial \ln \tilde{p}_{\mathcal{M}}(x, 0, z)}{\partial z} \right|_{z=0} \tag{2.19b}$$

are universal functions. The first of these functions has a simple form:

$$\tilde{p}_{\mathcal{M}}^{(1,0)}(x) \equiv x \tag{2.20}$$

a result which follows trivially by appeal to the Ising context (equation (2.11*a*)) together with the identity $\partial \ln p_L(\mathcal{M})/\partial h = L^d \mathcal{M}$. The second function is non-trivial: its form has (like that of $\tilde{p}_{\mathcal{M}}^{*}$) been established in earlier Monte Carlo studies of the Ising universality class [30]. Substituting (2.20) into (2.18) and appealing to (2.10*b*) we find

$$\langle u(\rho) \rangle - u_c \simeq r[\rho - \rho_c] + a_{\mathcal{E}} L^{-d+1/\nu} \tilde{p}_{\mathcal{M}}^{(0,1)}(a_{\mathcal{M}}{}^{-1} L^{\beta/\nu}[\rho - \rho_c]) \tag{2.21}$$

where r (equation (2.6)) controls the temperature dependence of the ('ordering') scaling field h, and thus the limiting critical slope of the coexistence curve which is identified by the condition $h = 0$ (figure 1).

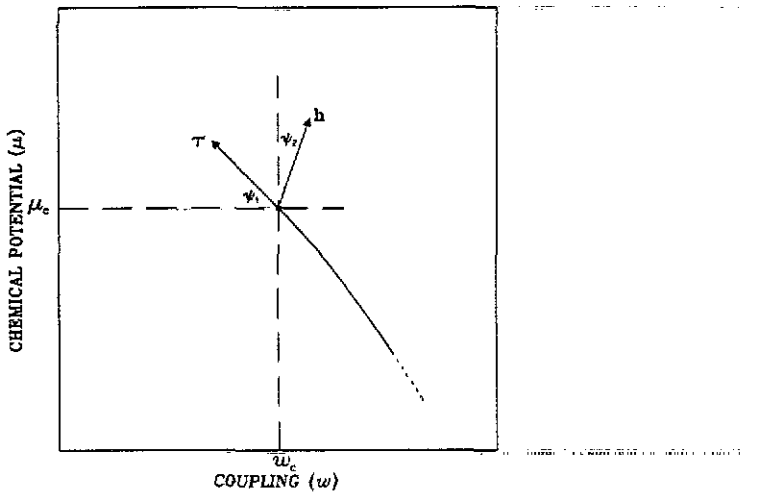

Figure 1. Schematic representation of the liquid–vapour coexistence curve showing the directions of the relevant scaling fields. The angles ψ_1 and ψ_2 are related to the field-mixing parameters s and r (equation (2.6)) by $-r = \tan\psi_1$ and $s = \tan\psi_2$.

Equation (2.21) provides a testable consequence of one form of field-mixing (a thermal contribution to the ordering scaling field). To demonstrate the distinctive consequences of the other form of mixing (the chemical potential contribution to the thermal scaling field) one needs to go beyond the approximations underlying equation (2.14). Returning to equation (2.13), and expanding in powers of the mixing parameter s we find that equation (2.14) may be refined to give

$$p_L(\rho) \simeq \Lambda_{\mathcal{M}}^{+} \tilde{p}_{\mathcal{M}}(\Lambda_{\mathcal{M}}^{+}[\rho - \rho_c], \Lambda_{\mathcal{M}} h, \Lambda_{\mathcal{E}} \tau) + \Delta p_L(\rho) \tag{2.22}$$

with

$$\Delta p_L(\rho) = -s \frac{\partial}{\partial \rho} \{[\langle u(\rho) \rangle - u_c - r(\rho - \rho_c)]\, p_L(\rho)\} + O(s^2) \tag{2.23}$$

so that, at criticality (appealing to equation (2.21))

$$\Delta p_L(\rho) \simeq \Lambda_{\mathcal{M}}^{+}\left[-s a_{\mathcal{E}} a_{\mathcal{M}}{}^{-1} L^{-(1-\alpha-\beta)/\nu}\right] \frac{\partial}{\partial x}\left\{\tilde{p}_{\mathcal{M}}^{(0,1)}(x)\tilde{p}_{\mathcal{M}}^{*}(x)\right\}_{x=a_{\mathcal{M}}{}^{-1}L^{\beta/\nu}[\rho-\rho_c]} \tag{2.24}$$

revealing the L-dependence anticipated in the argument we used to justify equation (2.14) as the leading contribution to the density distribution. This correction term explicitly captures the consequences of the field-mixing represented in the parameter s. Significantly, given the symmetries of $\tilde{p}_{\mathcal{M}}^{(0,1)}$ and $\tilde{p}_{\mathcal{M}}$ (both *even* in the scaling variable x), equation (2.24) also represents the leading contribution to the critical distribution that is *odd* in the scaling variable x. In what follows we shall see that, notwithstanding its status as a 'correction' to the leading behaviour, the existence and character of this contribution can be corroborated through simulation, by exploiting this symmetry—in much the same way as the related energy-like singularity in the coexistence curve diameter (equation (2.12)) is exposed by exploiting the symmetry-breaking that it represents.

3. Monte Carlo studies

3.1. Preliminaries

The Monte Carlo simulations described here were performed on the distributed array processors (DAPs) at the Edinburgh Parallel Computing Centre. We detail here the choices made in formulating the problem computationally.

We chose to implement a *geometrical* decomposition of the problem, to which the DAP architecture [36] is particularly well suited in two dimensions. With this strategy our two-dimensional space is partitioned into a square array of $\mathcal{L} \times \mathcal{L}$ square 'cells', the array as a whole being subject to periodic boundary conditions. Each 'cell' is in the charge of one processor in the sense that the coordinates of particles within the cell at any instant are handled by the corresponding processor. The mapping of the array of cells onto the array of processors involves the choice of two parameters: the size of the cell, a (in relation to the fundamental microscopic length-scale parameter σ, defined in equation (2.2)) and the linear dimension $\mathcal{L}$ of the array of cells.

The choice of a involves a compromise. If a is 'large' the number of particles per cell will be large, and the task of computing the interactions amongst the particles within one cell becomes a computationally intensive one, falling on a single processor. On the other hand, if a is 'small', a particle in one cell will interact with others in (many) distant cells, again making the task of identifying and calculating the interactions a demanding one. In practice we chose $a = r_c$, the Lennard-Jones cutoff, discussed later. This choice results in a mean number of approximately three particles per cell in the pure fluid phase and 1.5 particles in the coexistence region, while ensuring that interactions emanating from particles in one cell do not extend beyond the eight cells adjacent to it.

The characteristics of the processor array itself encourage choices of the form $\mathcal{L} = 2^n$, with $\mathcal{L} = 64$ as a formal upper limit. We chose to study the cases $\mathcal{L} = 8$ and $\mathcal{L} = 16$, containing respectively of order 100 and 400 particles at criticality, the latter proving to be the practical upper limit imposed by the need to cope with

critical slowing down. As the number of available processors (4096) exceeds the number of cells in both cases, we were able to study a number of independent systems simultaneously, thus considerably enhancing the rate of data acquisition after equilibration.

When simulating systems whose interaction potential decays rapidly with particle separation, it is usual to truncate the potential to reduce the computational effort. In the present work, we chose to truncate the Lennard-Jones potential at a distance $r_c = 2.0\sigma$. This cutoff lies at the lower end of the range of values to be found in the literature. Rovere *et al* [22, 23] chose $r_c = 2.5\sigma$; Singh *et al* [10] have $r_c = 10\sigma$. While surely of no consequence for universal characteristics of the critical behaviour, these differences have consequences for assignments of non-universal parameters, to which we will return.

Our Monte Carlo procedure itself has a Metropolis form, similar to that described by Adams for the grand canonical ensemble [37], but with two key differences. First our algorithm has a parallel form, permitting the simultaneous update of particles within different cells (subject to constraints that such particles do not interact). Second, we chose to implement only particle *transfer* (insertion and deletion), leaving particle *moves* to be performed implicitly as a result of repeated transfers. This choice is acceptable formally (it clearly realizes an ergodic system); it is also physically well motivated since it directs the computational effort at the density fluctuations, which are the bottleneck for configuration space evolution, the intrinsic inefficiency of particle insertion at high densities being compounded by the problems of critical slowing down. However we have not attempted to determine systematically whether this choice is optimal, given the current objectives. We note for future reference that the algorithm actually utilizes not the true (reduced) chemical potential μ featuring in equation (2.3) *et seq*, but an effective chemical potential μ^* to which the true chemical potential is related by

$$\mu = \mu^* + \mu_0 - \ln\left(N/\mathcal{L}^d\right) \tag{3.1}$$

where μ_0 is the chemical potential in the non-interacting (ideal gas) limit. It is this effective value that features in the results that follow. In a similar vein, we will also follow the convention according to which the system density is expressed as the mean number of particles, ρ^*, within the region defined by the Lennard-Jones potential parameter σ:

$$\rho^* = \rho\sigma^d = N\left[\sigma/\mathcal{L}a\right]^d . \tag{3.2}$$

Finally, for the observables to be recorded, we chose the distribution of the particle density $p_L(\rho)$ (identified in the first instance as a histogram of particle number), together with the energy density function $\langle u(\rho)\rangle$, identified as the mean value of the energy density (2.4*b*) for each value of ρ explored in the course of the simulation.

3.2. Equilibration and sampling considerations

Our principal concern in this work is with the behaviour on (or near) the liquid–vapour coexistence curve, and at the critical point in which it terminates. The metastable states associated with the former and the critical slowing down associated with the latter both result in extended equilibration times, the length of which

it is essential to gauge. To do so we carried out a series of test runs, in the vicinity of the coexistence curve (where equilibration problems are most acute), located in a manner to be described in the following section. The test runs each comprised a pair of simulation runs, each assigned identical model parameters, but different starting configurations. In the one case the run was started from a pure vapour configuration while in the other a pure liquid configuration was used. These initial configurations were themselves the product of preliminary runs performed well within the respective single phase regions. Over the course of each simulation we monitored the time evolution of the density distribution (and the mean density itself) by dividing each run into a number of consecutive measuring periods, each consisting of some 2×10^5 Monte Carlo steps *per cell* (MCS), and accumulating observations over each measuring period. Successive observations were separated by a number of intermediate MCS to reduce correlations in the data. Comparisons of the distributions built up over each period thus served to aid the identification of any systematic trends in the behaviour. The behaviour observed was found to depend on the system size, the initial configuration and the chosen position on the phase boundary. The essential points are made in figures 2 and 3, which illustrate respectively the problems of metastability and critical-slowing down. We discuss them in turn.

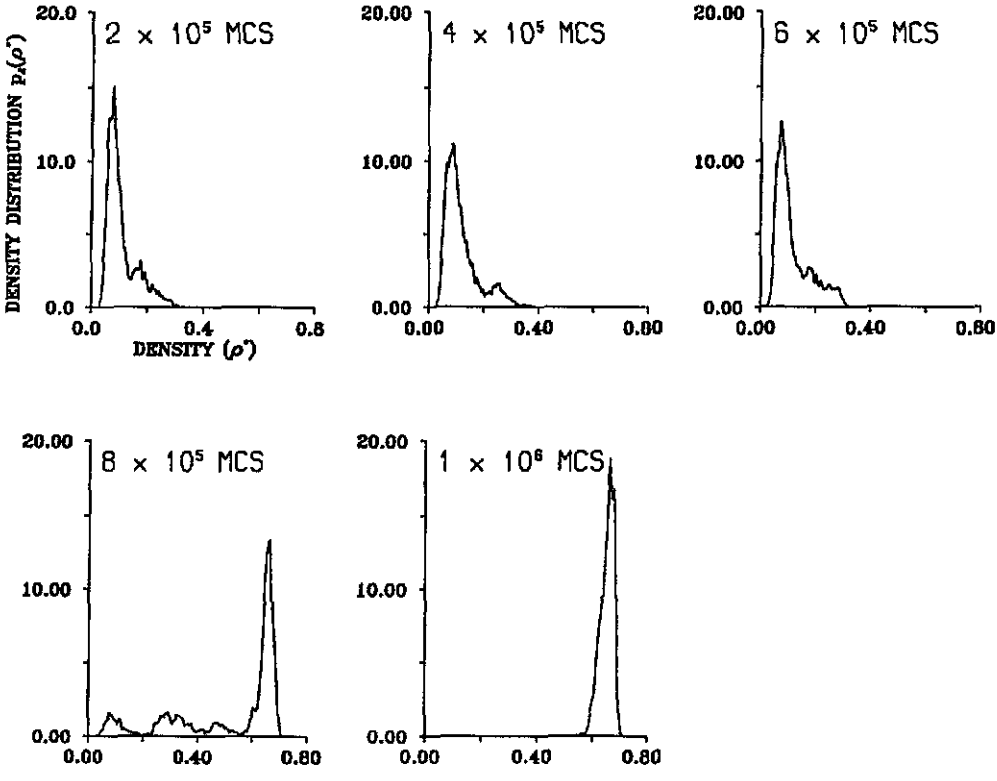

Figure 2. The time evolution of the density distribution of a $\mathcal{L} = 16$ system initially in a metastable vapour phase, at a temperature 1% below criticality.

Figure 2 shows the time evolution of the density distribution of a system (of size $\mathcal{L} = 16$) that lies close to coexistence at a temperature that is 1% below the

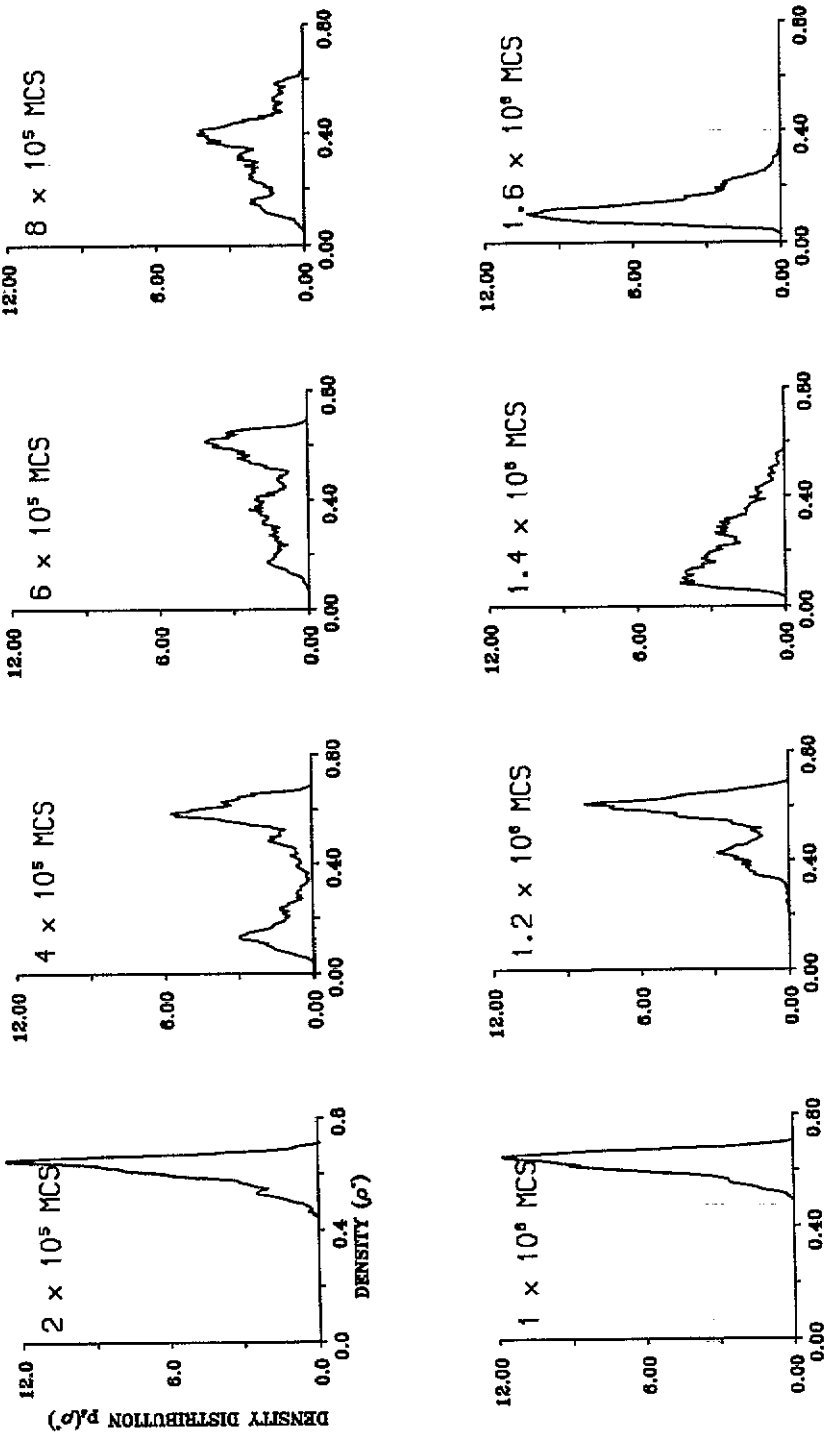

Figure 1. The time evolution of the density distribution of a $\mathcal{L} = 16$ system at criticality, showing the large slow fluctuations in the density.

critical temperature (whose location we discuss later). Each distribution represents data accumulated over a series of measuring periods, each of 2×10^5 MCS in duration. The initial state of the system lies in the pure vapour phase; the chemical potential slightly favours the liquid phase. The system remains in the metastable vapour phase for approximately 5×10^5 MCS before condensing, over a relatively short period, to the liquid phase where it remains. In this regime, the equilibration period (controlled by the extent of the potential period of metastability) was set at 1×10^6 MCS for the $\mathcal{L} = 16$ system (and 3×10^5 MCS for the $\mathcal{L} = 8$ system where metastability effects are less pronounced).

Figure 3 shows the time evolution of the density distribution very close to criticality (again for $\mathcal{L} = 16$), the data being gathered in the same fashion as described earlier. The density exhibits large and slow fluctuations between two still well-separated ranges which represent the vestiges of the coexisting phases. Typical critical configurations are shown in figure 4. In this regime, guided by the behaviour of the mean density, we utilized equilibration periods of 2.5×10^6 and 4×10^5 for $\mathcal{L} = 16$ and $\mathcal{L} = 8$ respectively. For both system sizes, the number of equilibration steps required in the region beyond the critical point was considerably less than in the critical region, decreasing systematically with increasing temperature.

The number of sample observations required to build a time-invariant distribution free of spurious structure, depends on the proximity to the critical point. For the $\mathcal{L} = 16$ system in the two-phase region, the data shown below typically involve 1×10^6 observations, each separated by 15 intermediate MCS. In the critical region we needed observation periods (long compared with the typical time-scale of the critical fluctuations) comprising up to 2×10^6 observations separated by 25 intermediate MCS. Observations times of approximately half these values were found to be adequate for the $\mathcal{L} = 8$ system.

3.3. Results

The computational problem posed by the location of the critical point in the fluid is substantially harder than its magnetic counterpart. In the (Ising) magnet the line of phase coexistence is prescribed by symmetry; in the fluid it has to be identified empirically, as a prelude to the location of the critical point in which it formally terminates. There are many possible computational criteria one may choose to effect this identification. Motivated by our central concern with the density distribution, we chose to adopt the criterion that the line of phase coexistence is the set of points (more precisely, as discussed later, a *subset* of those points) in $\mu - w$ space along which the density distribution displays two peaks of equal height: this condition represents [33] the finite-size analogue of the free-energy equality that characterizes the phase boundary in the thermodynamic limit. In finding and tracking this set of points we made substantial use of the *derivatives* of the density distribution with respect to the two control parameters μ and w. The derivative with respect to w is provided by the energy function measured in the simulation (cf equation (2.17*b*)); the derivative with respect to μ is trivially related to the distribution itself (equation (2.17*a*)). Appeal to these derivatives provides initial estimates (subsequently refinable) for the changes in μ and w that, together, preserve the equality of heights of the two peaks.

Implementing this strategy we identified the set of $\mu^* - w$ values (recall equation (3.1) for the definition of μ^*) shown in figure 5. The results for $\mathcal{L} = 8$ and $\mathcal{L} = 16$ are fully consistent with one another to a high precision: the value of μ^* (for a given w) fulfilling the equal-height criterion is identifiable to four significant

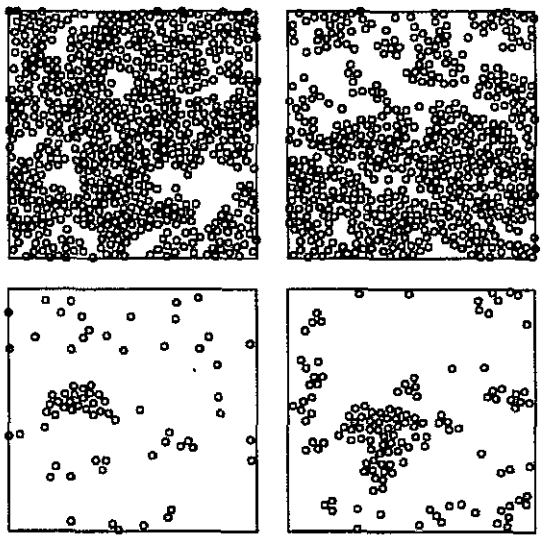

Figure 4. Typical particle configurations of the $\mathcal{L} = 16$ system at criticality.

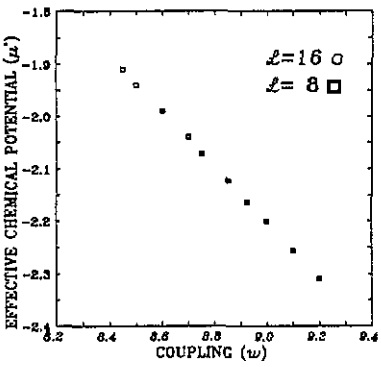

Figure 5. The measured line of pseudo-coexistence defined by the set of points in $\mu^* - w$ space for which the density distribution, measured for $\mathcal{L} = 8$ and $\mathcal{L} = 16$, has two peaks of equal height. The uncertainties in the assignments of μ^* for a given w are substantially smaller than the symbol sizes.

figures in the $\mathcal{L} = 8$ system; with $\mathcal{L} = 16$, it is identifiable (at substantially more computational cost) to five significant figures.

The density distributions associated with a subset of these points are shown in figures 6(*a*) and 6(*b*), for $\mathcal{L} = 8$ and $\mathcal{L} = 16$ respectively. Two distinct types of crossover behaviour (with increasing $\mathcal{L}$) are discernible.

For strong enough couplings the change from $\mathcal{L} = 8$ to $\mathcal{L} = 16$ is accompanied by a sharpening of the double-peaked character of the distribution. This is consistent with the expected behaviour on the line of phase coexistence, which should asymptotically (for large enough system size $\mathcal{L}$) show two Gaussians centred on the densities of the two coexisting phases. On the other hand, for weaker couplings, the change from $\mathcal{L} = 8$ to $\mathcal{L} = 16$ is accompanied by a broadening of the two peaks, and a transfer of weight into the central portion of the distribution. This is indicative of single-phase behaviour, where the limiting distribution will be a single Gaussian.

On this basis one can see immediately from a comparison of figures 6(*a*) and 6(*b*) that couplings w of 8.925 or below are subcritical while those of 9.1 or above

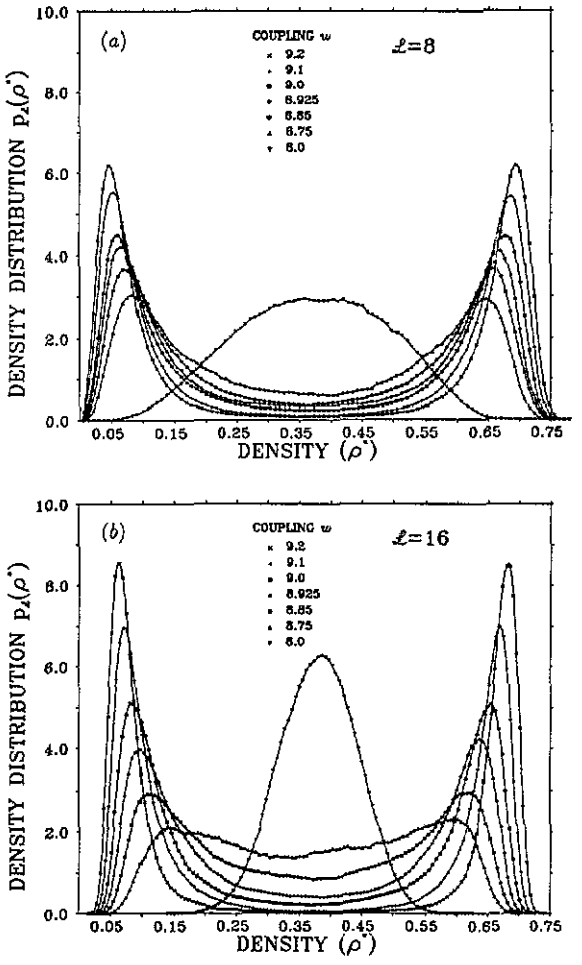

Figure 6. The fluid density distributions in systems of sizes (*a*) $\mathcal{L} = 8$ and (*b*) $\mathcal{L} = 16$, for a variety of couplings w along the line of pseudo-coexistence, identified in figure 5. The statistical uncertainties are smaller than the symbol sizes; the curves are simply guides to the eye.

are supercritical. Thus the majority of the points shown in figure 5 actually identify not the coexistence curve itself but the continuation of it that persists in finite-size systems.

The critical point itself is formally identifiable as the point on this 'pseudo'-coexistence curve that separates these two different forms of crossover. The coupling which we have identified as coming closest to realizing this critical state is $w_c = 9.00$. The evidence supporting this assignment is as follows.

First, given an appropriate choice of the non-universal scale factor $a_{\mathcal{M}}$, the associated $\mathcal{L} = 16$ density distribution can be mapped into very close correspondence with the universal function $\tilde{p}_{\mathcal{M}}$ (equation (2.15)), prescribed in earlier studies of members of the Ising universality class [30]. This mapping is shown in figure 7. The extent of the agreement is a *motivation* for our assignment of the critical coupling (made specifically to optimize this mapping) rather than further *corroboration*. However, the fact that it is possible at all, provides clear support for the general framework

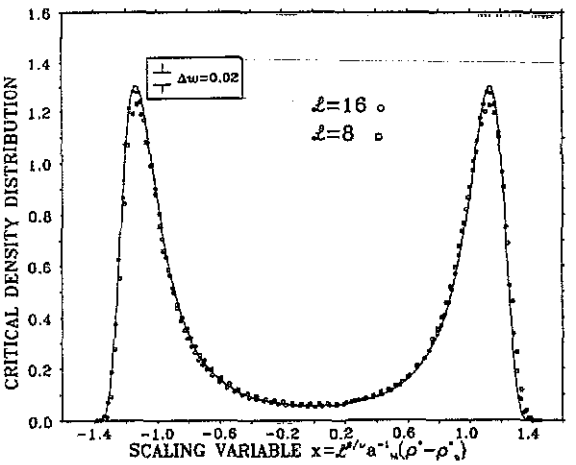

Figure 7. The fluid density distributions for $\mathcal{L} = 8$ and $\mathcal{L} = 16$ at criticality ($\mu_c^* = -2.202$, $w_c = 9.00$) expressed as functions of the scaling variable $x \equiv \mathcal{L}^{\beta/\nu} a_{\mathcal{M}}^{-1}[\rho^* - \rho_c^*]$ The full curve is the fixed point function $\tilde{p}^*_{\mathcal{M}}(x)$ appropriate for the Ising universality class [30]. The non-universal scale factor $a_{\mathcal{M}}$ is chosen so that, for $\mathcal{L} = 16$, the scaling variable x has unit variance, consistent with the conventions implicit in the definition of $\tilde{p}^*_{\mathcal{M}}(x)$. The value of β/ν implicit in the horizontal scale is $\beta/\nu = 0.125(1)$. The inset shows the size of the change in height of the $\mathcal{L} = 16$ distribution peaks resulting from a change $\Delta w = 0.02$ along the line of pseudo-coexistence.

advanced here, linking the fluid and Ising magnet.

The consistency of the picture is further supported by the near-scaling behaviour evident at this near-critical point: figure 7 also shows the corresponding distribution for the $\mathcal{L} = 8$ system, plotted as a function of the appropriate scaling variable with the same assignment of the scale factor $a_{\mathcal{M}}$, and with the index β/ν assigned so that this distribution (like the others shown) has unit variance. The value required to satisfy this criterion is $\beta/\nu = 0.125(1)$, in embarrassingly good correspondence with the exact Ising limit $\beta/\nu = \frac{1}{8}$. Although the differences from the universal limiting form are quite apparent for the $\mathcal{L} = 8$ system, they are quite comparable in size and (at first sight) also in form with discrepancies found in the analysis of ϕ^4 models [38] which were subsequently shown to be attributable to corrections to scaling. We shall see, however, that they contain further structure of a significantly different form.

The remaining evidence in support of our location of criticality comes from our measurements of the energy function $\langle u(\rho) \rangle$. Figure 8 shows the results for our two system sizes at criticality. According to our proposed scaling form (2.21) this function consists of two terms, the one explicitly *odd* (linear) in the scaling variable, and the other (as consideration of the Ising limit shows) *even*. The two components may thus be identified by exploiting these different symmetries. The result for the odd (and asymptotically dominant) component of the energy function is expressed in the assignment $r = -0.529(2)$, which is consistent with the value obtained from the measured slope of the coexistence curve. The results for the even (sub-dominant) contribution to the energy function are expressed in figure 9. The smooth curve represents the result for the function $\tilde{p}^{(0,1)}_{\mathcal{M}}$ established in earlier studies of the Ising universality class [30]. The data points represent the symmeterized energy function

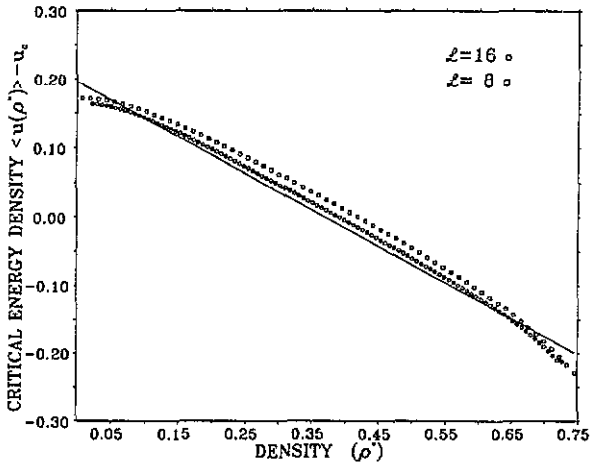

Figure 8. The fluid energy density for $\mathcal{L} = 8$ and $\mathcal{L} = 16$ at criticality. The full curve (cf equation (2.21)) is of the form $r[\rho^* - \rho_c^*]$ where, from the measured slope of the pseudo-coexistence curve (figure 5) $r = -0.529(2)$.

u^s defined by

$$u^s(\langle\rho\rangle \pm \Delta\rho) = (2a_\mathcal{L})^{-1}\mathcal{L}^{d-1/\nu}\langle\{u(\langle\rho\rangle + \Delta\rho) + u(\langle\rho\rangle - \Delta\rho) - 2u(\langle\rho\rangle)\}\rangle \quad (3.3)$$

which represents the 'even' part of the left-hand side of equation (2.21) with u_c and ρ_c replaced by their finite-size equivalent forms. This is one way of coping with 'corrections' to equation (2.21); it has the merit that, in this amended form, equation (2.21) satisfies the sum rule that follows on integration with respect to ρ. The collapse shown is effected with the assignment of the single non-universal scale factor $a_\mathcal{L}$ together with a value $1/\nu = 1.03(3)$, to be compared with the Ising value $\nu = 1$. While the agreement as regards the index is satisfactory, we believe that here (as in figure 7) the *scaling function* represents a substantially more compelling signature of the universality class.

This general point is made in an even more striking way in the context of the *corrections* to scaling, manifesting themselves in the differences between the measured density distributions and their limiting Ising form (cf figure 7). There are, in fact, four sources for such discrepancies. Differences between the assigned and true values of w_c and μ_c, are responsible for two of these, giving rise (to the extent that they exist) to two *relevant* corrections, associated with (not-quite-zero) values of h and τ. The third source of discrepancies is the leading *irrelevant* scaling field associated with the Ising universality class, which is not included in the scaling *ansatz* (2.10*a*). Finally, there is the correction arising from scaling-field-mixing, identified in equation (2.24). Identifying the latter correction amidst the others seems an unlikely proposition. There are a number of reasons why it does actually prove possible.

The first is the *symmetry* of the correction (2.24), which is *odd* in $\rho - \rho_c$. One may thus antisymmetrize the measured distribution about its median point to eliminate the corrections associated both with the leading irrelevant correction to scaling and the even contribution associated with the thermal scaling field τ.

The second mitigating circumstance is that the functional forms of the two anti-symmetric corrections are independently known. The correction due to a non-zero

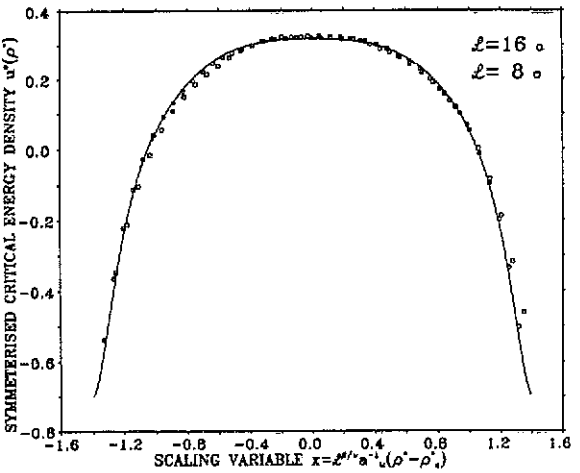

Figure 9. The critical fluid energy density for $\mathcal{L} = 8$ and $\mathcal{L} = 16$ symmetrized about ρ_c^* and scaled as prescribed in equation (3.3), compared with the function $\tilde{p}_{\mathcal{M}}^{(0,1)}$ appropriate to the Ising universality class (full curve). The horizontal scale is identical to that featuring in figure 7. The non-universal scale factor $a_{\mathcal{E}}$ has been chosen so that the $\mathcal{L} = 16$ data and the Ising form match at $x = 0$. The value of $1/\nu$ implicit in the vertical scale is $1/\nu = 1.03(3)$.

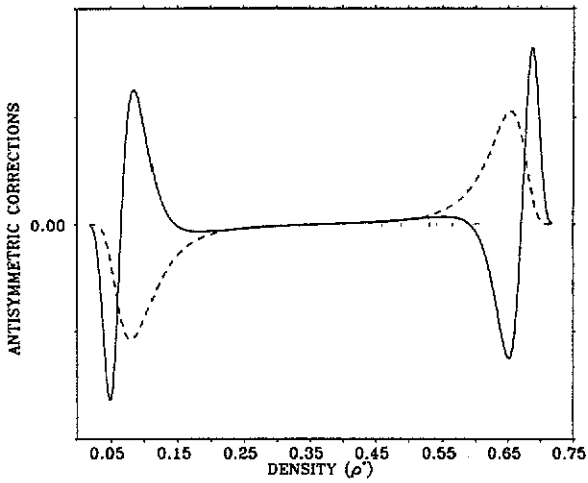

Figure 10. The structure of the two antisymmetric corrections to the near-critical density distribution. The full curve shows the form arising from the field-mixing (equation (2.24)). The broken curve shows the form associated with a small non-zero ordering field h (equation (2.19*a*)).

h is controlled by the function $\tilde{p}_{\mathcal{M}}^{(1,0)}$ (equation (2.19*a*)); the correction due to field-mixing is prescribed in equation (2.24). Both correction forms are thus determined by the results of Ising model studies. Figure 10 shows that they have quite distinct signatures. A little thought then shows that our measured distribution must have contributions from both of these sources (if it has a contribution from either) since mutual cancellation must occur to satisfy the equal-peak-height criterion imposed to locate coexistence and criticality. The latter criterion thus imposes a constraint on the proportion of the two contributions. To determine the underlying contribution associ-

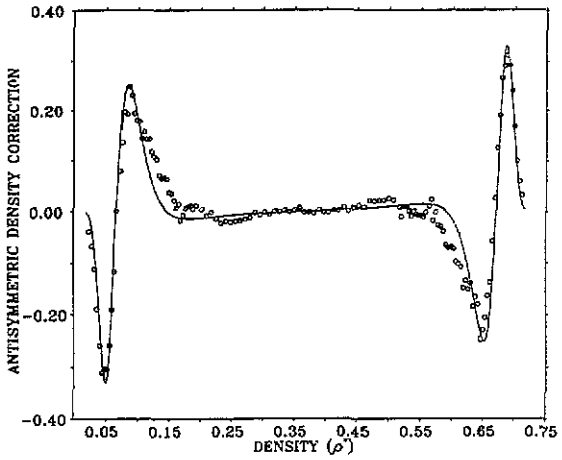

Figure 11. The measured antisymmetric correction to the $\mathcal{L} = 16$ distribution (figure 7), itself corrected for a small off-coexistence contribution, as described in the text, and shown as the data points; the full curve represents the prediction following from equation (2.24), utilizing pre-determined Ising forms [30].

ated with the field-mixing, one may thus identify the antisymmetric contribution to the measured distribution, and then remove from it the contribution due to departures from coexistence (consistent with the noted constraint). The results of applying this procedure to the measured $\mathcal{L} = 16$ distribution (figure 7) are shown in figure 11. The correction made to account for departures from coexistence corresponds to a shift in our assigned μ_c by an amount ($-0.000\,13$ to be precise) small compared with the uncertainties (see later) associated with the location of the critical point *along* the line of pseudo-coexistence. The resulting agreement with the predicted form is excellent, providing striking corroboration of the mixed-scaling-field theory. The single scale factor required to effect this mapping implies a value $s = -0.24(3)$ for the parameter describing the more significant of the two forms of scaling field-mixing.

To conclude this section we summarize our assignments of the critical parameters, together with their error bounds. Defining (in accordance with convention) $T_c^* \equiv 4/w_c$ and recalling the other notation established in equations (3.1) and (3.2) we assert:

$$T_c^* = 0.44 \pm 0.005 \qquad \mu_c^* = -2.20 \pm 0.04 \qquad \rho_c^* = 0.368 \pm 0.003. \tag{3.4}$$

The value of μ_c^* is tied (by our tightly defined line of pseudo-coexistence) to the value of w_c; the value of ρ_c^* is both the mean and median of the critical density distribution. The discussion of these assignments and uncertainties features in our concluding section.

4. Conclusions

The general thesis motivating this work is that the fluid critical-point problem should and can be more fully integrated with its magnetic counterpart. This thesis has both a philosophical and a practical element. In a philosophical vein we wished to demonstrate more explicitly that (and the *sense* in which) the fluid and the magnet

belong to the same universality class. In a practical vein we set out to explore whether the computational framework deployed so successfully in studies of magnetic systems could be generalized to yield more productive ways of simulating near-critical fluids.

The first of these objectives is, we believe, convincingly fulfilled in figures 7 and 9. These figures bear out our general scaling form (2.10*a*) and the picture it expresses: the near-critical patterns of the fluid density fluctuations match those of the magnetization fluctuations in the Ising ferromagnet.

As regards the general computational issues, we believe that the methods we have presented have proved materially more successful than those of our predecessors: the uncertainties associated with the critical-point parameters assigned in equation (3.4) represent a significant improvement on the error bounds cited by others (at least, those who cite *any*). Moreover, the uncertainties cited in (3.4) are, we believe, conservative. Thus, the range of coupling values consistent with the quoted uncertainties extend to two values ($u = 9.1$ and $u = 8.925$) on either side of our designated critical value (cf figures 6(*a*) and 6(*b*)) which are certainly sub- and super-critical respectively. In fact, if we were to *assume* that finite-size corrections die out with $\mathcal{L}$ at the rate suggested by comparison of our $\mathcal{L} = 8$ and $\mathcal{L} = 16$ 'critical' data, the requirement (then largely rationalized) that the $\mathcal{L} = 16$ distribution should match the Ising form provides substantially tighter bounds on the critical parameters. The point is illustrated by the inset in figure 7 which shows the sensitivity of the measured $\mathcal{L} = 16$ distribution to changes in the control parameters. Specifically, the inset shows the change in the height of the $\mathcal{L} = 16$ distribution peaks resulting from a change in the coupling w of $|\Delta w| = 0.02$ corresponding (cf the units introduced in (3.4)) to a change of only $k\Delta T = 0.001$ along the line of pseudo-coexistence (i.e. with μ^* also changed so as to maintain the equal-height criterion). The potential sensitivity of the method should be apparent. Indeed it should be apparent *a priori*: one *must* fare better in searching for criticality if one's guide is the matching of a readily measurable *function* to an *independently known* form appropriate for a *finite-size system*, than if one has to extrapolate a power law that is finite-size limited and makes use of only a fragment of the data available from the simulation.

Turning to the critical parameters themselves, we note that, in the same units as those employed in equation (3.4) Tsien and Valleau [7] suggest T_c^* between 0.625 and 0.7, Henderson [8] gives $T_c^* = 0.56$, Barker *et al* [9] quote $T_c^* = 0.52$, Rovere *et al* [23] suggest $T_c^* = 0.50 \pm 0.02$ while Singh *et al* [10] quote $T_c^* = 0.472$. Comparisons amongst these assignments, and with our own estimate, are complicated by differences in the value assigned to the Lennard-Jones cutoff, whose effect on the critical parameters is significant, a point emphasized by Smit and Frenkel [39]. One can estimate the extent of the consequences of the different cutoff assignments by utilizing the implied values of the second virial coefficient to give the associated van der Waals transition temperature. Making the reasonable approximation† that the fractional change in the true critical temperature (arising from a change in the cutoff) matches the fractional change in the van der Waals transition temperature, we find, for example, that the difference between the cutoff ($r_c = 2.5\sigma$) employed by Rovere *et al* [23] and our own choice ($r_c = 2\sigma$) accounts for approximately one-third of the difference between their assignment of the critical temperature and

† This approximation reproduces rather well the *difference* reported in [39] between the transition temperature of a system described by the full potential and a system with a potential both truncated and shifted.

our own, leaving a discrepancy which we believe is significant. Thus we believe that virtually all previous studies have significantly overestimated the critical temperature, presumably because (without the insights offered in this work) it is all too easy to mistake the finite-size extension of the coexistence curve for the real thing. This point has also been made recently by Mon and Binder [40] in a critique of Monte Carlo studies of phase coexistence using the Gibbs ensemble: the point at which the 'densities' (however identified) of the two coexisting phases merge in a finite system can constitute a serious overestimate of the critical point, the effect being particularly pronounced in two dimensions. It is thus a little hard to understand the relatively good agreement between our estimate of the critical temperature and that of Singh *et al* [10] on the basis of just such a Gibbs ensemble study, with no analysis of finite-size effects. Indeed Smit and Frenkel [39] have repeated the Gibbs ensemble calculations and analysis of Singh *et al*, with the result $T_c^* = 0.515 \pm 0.002$ which *does* display the expected overestimate (with respect to our own work).

Turning to the distinctive respects in which the fluid *differs* from the Ising magnet, we note that the results for the energy function (figure 9) bear out equation (2.21), and thus corroborate one aspect of our generalized scaling theory (equation (2.10*a*)), namely the manner in which the *temperature* features in the ordering scaling field h (equation (2.6)). More significantly, we have seen that the second kind of field-mixing (the fact that the *chemical potential* features in the *thermal* scaling field τ) has a quite distinctive signature in the antisymmetric corrections to the limiting form of the critical density distribution. This success is further testimony to the power† of the methods advanced here. Experiments on fluids have found it difficult to demonstrate this mixing through the resulting non-analytic contribution to the t-dependence of the coexistence curve diameter (2.12); any Monte Carlo procedure that simply tries to emulate such experiments would surely fail. The present procedure circumvents these problems by using the additional information on a whole range of scaling functions directly accessible to Monte Carlo techniques.

Finally we remark that if one wishes to refine the simulation results presented here, one must certainly find a way of handling larger system sizes. While growing computational power may make such studies feasible, some advances at an algorithmic level are clearly called for. The algorithm underlying this work suffers from two well known problems: the intrinsic inefficiency of particle exchange with a *dense* system; and the problem of critical slowing down. One method for improving the acceptance rate in the grand canonical ensemble has been suggested [41]. However it would appear that collective (cluster) updating schemes [42] hold the greatest promise for tackling critical slowing down. Their extension to off-lattice problems is the subject of ongoing study.

Acknowledgment

NBW acknowledges the financial support of a Science Faculty scholarship from The University of Edinburgh.

† The mixing is, however, implicit in the parameterization of the equation of state. Our results for the mixing parameter s is consistent in both sign and magnitude with the typical values implied by such measurements on three-dimensional fluids [3].

References

[1] Kadanoff L P 1976 *Phase Transitions and Critical Phenomena* ed J C Domb and M S Green (New York: Academic) ch 1, pp 1–34
[2] Ley-Koo M and Green M S 1981 *Phys. Rev.* A **23** 2650
[3] Sengers J V and Levelt Sengers J M H 1986 *Ann. Rev. Phys. Chem.* **37** 189
[4] Nicoll J F 1981 *Phys. Rev.* A **24** 2203
[5] Nicoll J F and Zia R K P 1981 *Phys. Rev.* B **23** 6157
[6] Zhang Q and Badiali J P 1991 *Phys. Rev. Lett.* **67** 1598
[7] Tsien F and Valleau J P 1974 *Mol. Phys.* **27** 177
[8] Henderson D 1977 *Mol. Phys.* **34** 301
[9] Barker J A, Henderson D and Abraham F F 1981 *Physica* A **106** 226
[10] Singh R R, Pitzer K S, de Pablo J J and Prausnitz K M 1990 *J. Chem. Phys.* **92** 5463
[11] Rehr J J and Mermin N D 1973 *Phys. Rev.* A **8** 472
[12] Weiner J, Langley K H and Ford N C Jr 1974 *Phys. Rev. Lett.* **32** 879
[13] Greer S C, Das B K, Kumar A and Gopal E S R 1983 *J. Chem. Phys.* **79** 4545
[14] Jungst S, Knuth B and Hensel F 1985 *Phys. Rev. Lett.* **55** 2167
[15] Singh R R and Pitzer K S 1990 *J. Chem. Phys.* **92** 3096
[16] Narger U and Balzarani D A 1990 *Phys. Rev.* B **42** 6651
[17] Goldstein R E, Parola A, Ashcroft N W, Pestak M W, Chan M W H, de Bruyn J R and Balzarini D A 1987 *Phys. Rev. Lett.* **58** 41
[18] Goldstein R E and Parola A 1988 *J.Chem. Phys.* **88** 7059
[19] Pestak M W, Goldstein R E, Chan M W H, de Bruyn J R, Balzarini D A and Ashcroft N W 1987 *Phys. Rev.* B **36** 599
[20] Reatto L, Meroni A and Parola A 1990 *J. Phys.: Condens. Matter* **2** SA121
[21] Parola A and Reatto L 1985 *Phys. Rev.* A **31** 3309
[22] Rovere M, Heermann D W and Binder K 1988 *Europhys. Lett.* **6** 585
[23] Rovere M, Heermann D W and Binder K 1990 *J. Phys.: Condens. Matter* **2** 7009
[24] Binder K 1981 *Z. Phys.* B **43** 119
[25] Binder K and Heermann D W 1988 *Monte Carlo Simulation in Statistical Physics* (Berlin: Springer)
[26] Bruce A D and Wilding N B 1992 *Phys. Rev. Lett.* **68** 193
[27] Kim H K and Chan M W H 1984 *Phys. Rev. Lett.* **53** 170
[28] Wegner F J 1972 *Phys. Rev.* B **5** 4529
[29] Bruce A D 1981 *J. Phys. C: Solid State Phys.* **14** 3667
[30] Nicolaides D and Bruce A D 1988 *J. Phys. A: Math. Gen.* **21** 233
[31] Eisenriegler E and Tomaschitz R 1987 *Phys. Rev.* B **35** 4876
[32] Landau L D and Lifshitz E M 1980 *Statistical Physics* (New York: Permagon) part 1
[33] Challa M S S, Landau D P and Binder K 1986 *Phys. Rev.* B **34** 1841
[34] McCoy B M and Wu T T 1973 *The Two-dimensional Ising Model* (Harvard: Harvard University Press)
[35] Huse D A and Fisher M E 1982 *J. Phys. C: Solid State Phys.* **15** L585
[36] Wilding N B, Trew A S, Hawick K A and Pawley G S 1991 *Proc. IEEE* **79** 574
[37] Adams D J 1975 *Mol. Phys.* **29** 307
[38] Bruce A D 1985 *J. Phys. A: Math. Gen.* **18** L873
[39] Smit B and Frenkel D 1991 *J. Chem. Phys.* **94** 5663
[40] Mon K K and Binder K 1991 *Preprint* Mainz
[41] Mezei M 1980 *Mol. Phys.* **40** 901
[42] Swendsen R H and Wang J S 1987 *Phys. Rev. Lett.* **58** 86